

# Combined Dispersion and Reflection Effects at Sloping Structures

Fritz Büsching

Prof. Dr.-Ing. Head Hydraulics Laboratory  
Bielefeld University of Applied Sciences  
Diesselhorststr. 01, 38116 Braunschweig, Germany  
buesching@hollow-cubes.de

## Abstract

Model investigations have been executed in using irregular waves acting on smooth sloping structures inclined 1:3. Analyzing composite spectra in front of the structure the following results are found: (1) A set of partial standing waves is present in front of the structure coincidentally. (2) Each partial clapotis is composed of a number of bound frequency components disposing of an anomalous dispersion property. (3) Reflection coefficients increase with the frequency decreasing. (4) Component clapotis waves are shifted in the upslope direction with frequency increasing. (5) Relative shift of superimposed component clapotis is in accordance with increasing asymmetry of breaking waves.

## 1 Introduction

Model investigations on new designed (patented) hollow sloping structures have been executed in the Hydraulic Laboratory of Bielefeld University of Applied Sciences since 1990. Such tests included "Hollow Cubes" forming a *one layer* system as well as a *stepped structure* constructed by *two layers*. In both cases a more or less smooth conventional slope face was used as a reference. There are examples of stepped hollow structures reducing the wave energy (calculated from spectra of vertical water level deflections) in front of a slope by more than 65% (at the breaker position) compared to that on a smooth slope, see [8], [10]. The detailed results on irregular water level deflections and on monochromatic waves synchronously measured in front of the smooth and the hollow sloping structures of scale 1:5 and slopes  $1:0 \geq 1:n \geq 1:3$  had been published previously by the author in [3], [4], [5], [6] and [8].

In order to demonstrate the advantages of such hollow structures versus a more or less smooth slope, water level deflections and / or water pressures were measured quasi synchronously at a number of gauge stations in front of the two slopes.

The present contribution, however, is oriented preferably on the methods of evaluation used and on some general findings on spectrum reflection resulting from that special technique of analysing composite spectra.

In the following special reference is made to the measurements at 1:3 slope structures reported in [3]. Because

of the lack of space here, reference can be made, however, to the *smooth slope only*. Calculations, some of the graphs are based on, had been performed by Hagemeyer and Kramer (1992)[9].

## 2 Model Investigations

Because of the water depth conditions to be considered in the wave flume, an input wave spectrum was used, similar to those measured near the breaker zone of Sylt Island/North Sea [7]. Hence, in the model input spectrum the energy densities are concentrated around a median frequency  $f = 0.56$  Hz.

In this particular case tests had been carried out comprising a rather big number of 90 wave probe stations equally spaced 10 cm in the perpendicular line in front of each slope. The signals from the wave probes were recorded quasi synchronously and were processed by spectrum analyses confined to a total frequency range of 0.0326 to 1.3997 Hz.

As there are water level deflections of oncoming and reflected waves superimposed at any gauge station, the spectra calculated represent *composite spectra*. Typical diagrams further analysed in the remainder of this presentation show values of the integrated spectrum area IA (variance) plotted along with the gauge station distance from the slope, i.e., from the point IP of the stillwater level (SWL) intersecting the slope, which is also sketched in relation to the probe stations at the bottom of Fig.01. Because the variance is proportional to the wave energy (of vertical water level deflections) contained in the respective frequency range, changes in those plots can be interpreted with respect to the actual position and dominance of partial clapotis in relation to the sloping structure. In Fig.01 the variation in the plot of the total energy indicates that the length of a "resultant clapotis" is about  $L_C = 3.65$ m (distance between the first and the third minimum of energy). Although there are some disturbances to be seen in the plot, it will be shown that conclusions of some quality can be drawn from that data, provided that the total frequency range is subdivided into a number of smaller frequency ranges and noise frequency ranges are disregarded.

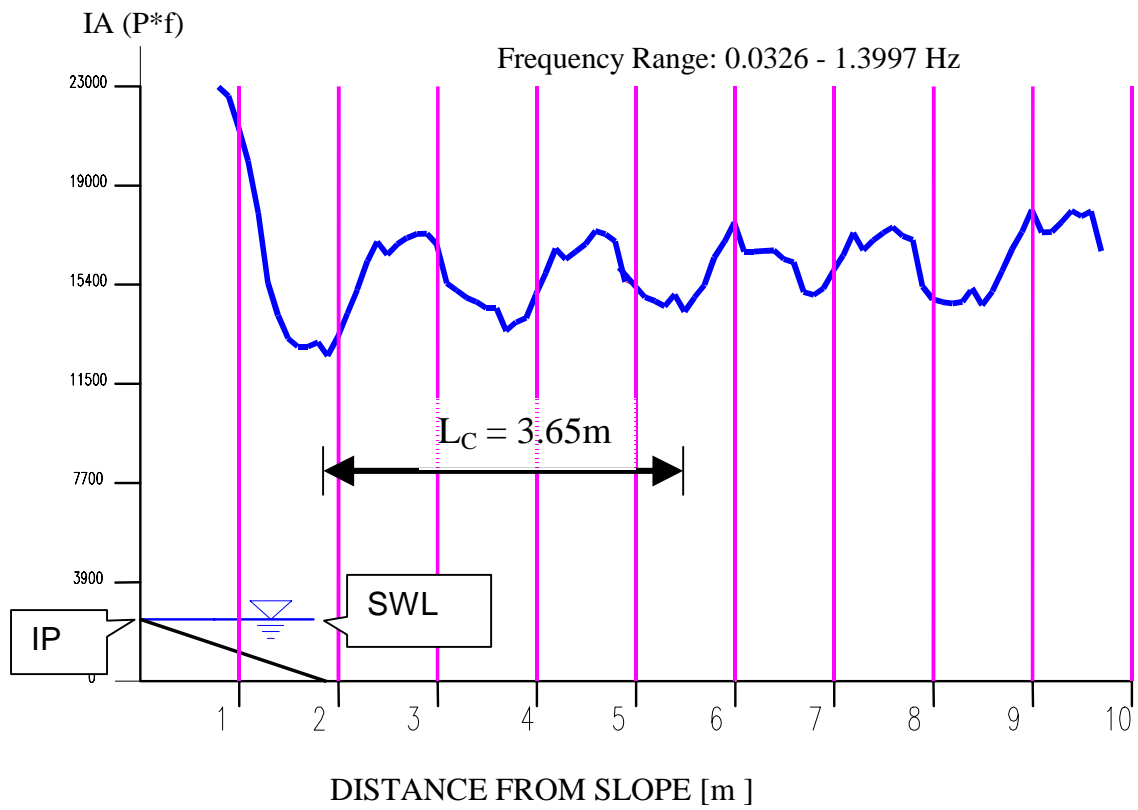


Fig.01: Total Energy in Front of a Smooth Slope 1:3

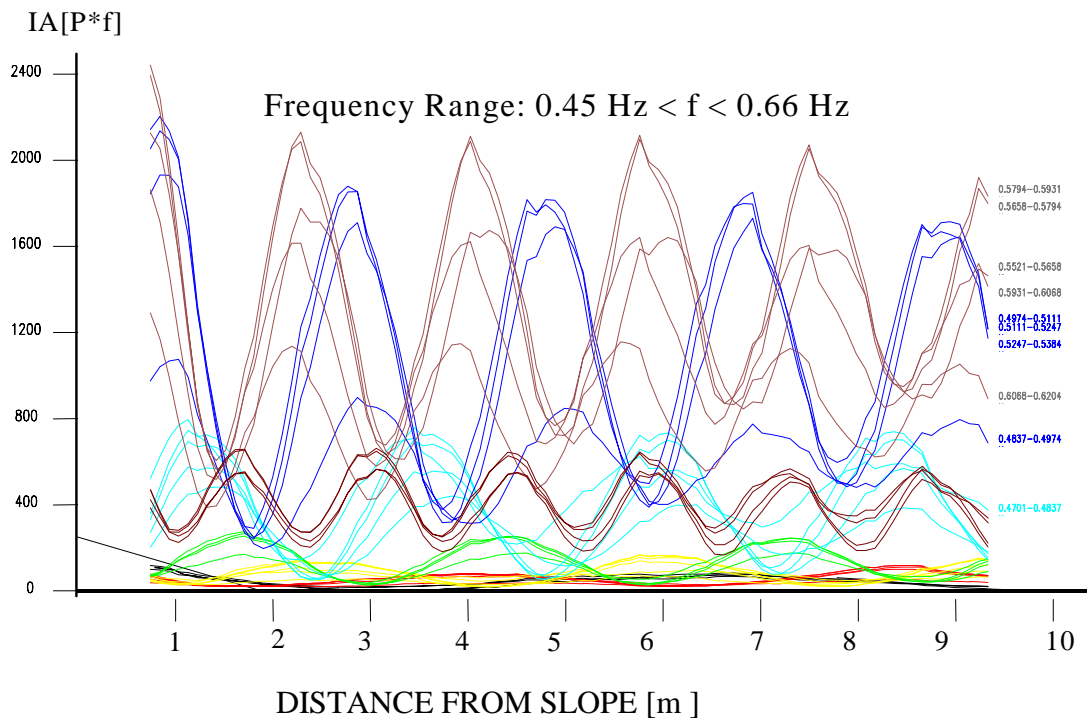


Fig.02: Energy Content of a big Number of Frequency Components

Plotting the energy contents of a rather big number of very small frequency increments  $\Delta f$  separately, it can be seen that some of those incremental frequencies possess similar energy distributions in the length scale in relation to the distance from the sloping structure (point IP), i.e., they have *same* distances between neighbouring energy minima or neighbouring energy maxima respectively, see Fig.02.

Obviously such bound component waves disposing of equal wave lengths  $L$  must obey an anomalous dispersion law, since - at a given water depth  $d$  - phase velocity

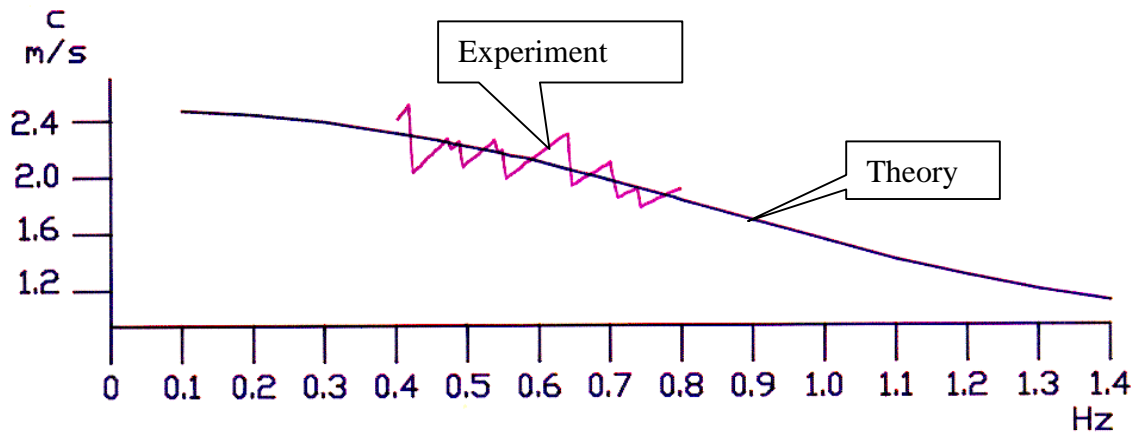


Fig.03: Anomalous Dispersion of Energy Containing Bound Frequencies

Obviously such bound component waves disposing of equal wave lengths  $L$  must obey an anomalous dispersion law, since - at a given water depth  $d$  - phase velocity

$c = L \cdot f$  increases with frequency. In Fig.03 such phase velocities are plotted together with the respective curve according to the classical dispersion relation.

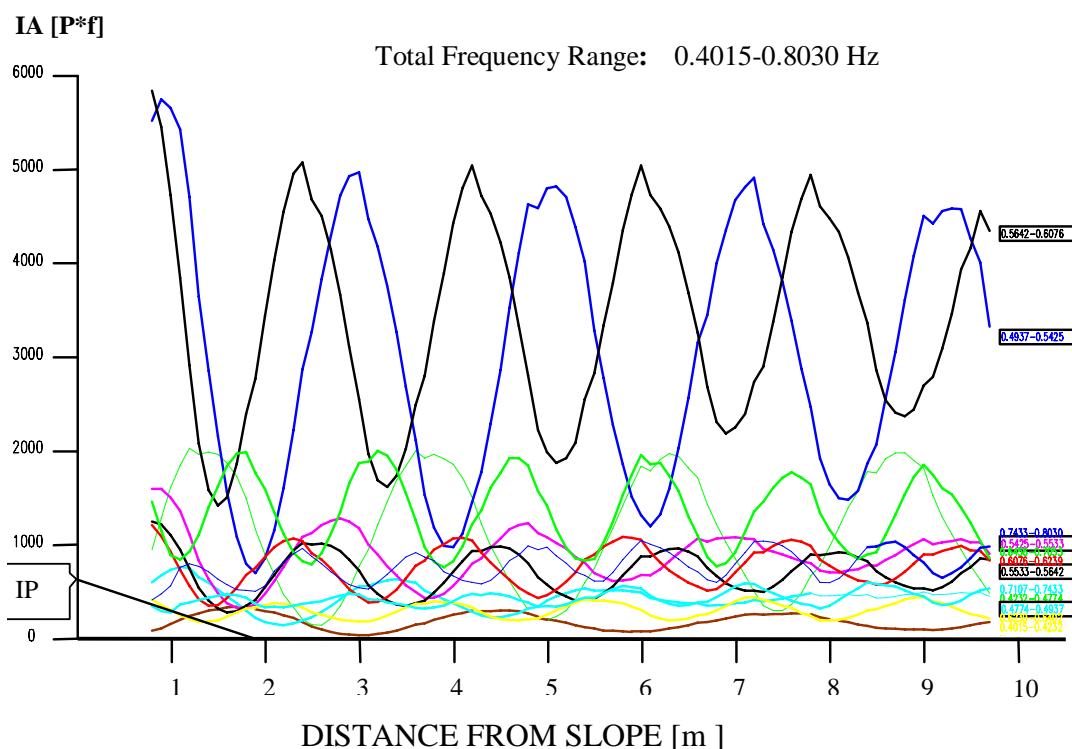


Fig.04: Clapotis Energy of Bound Frequency Components

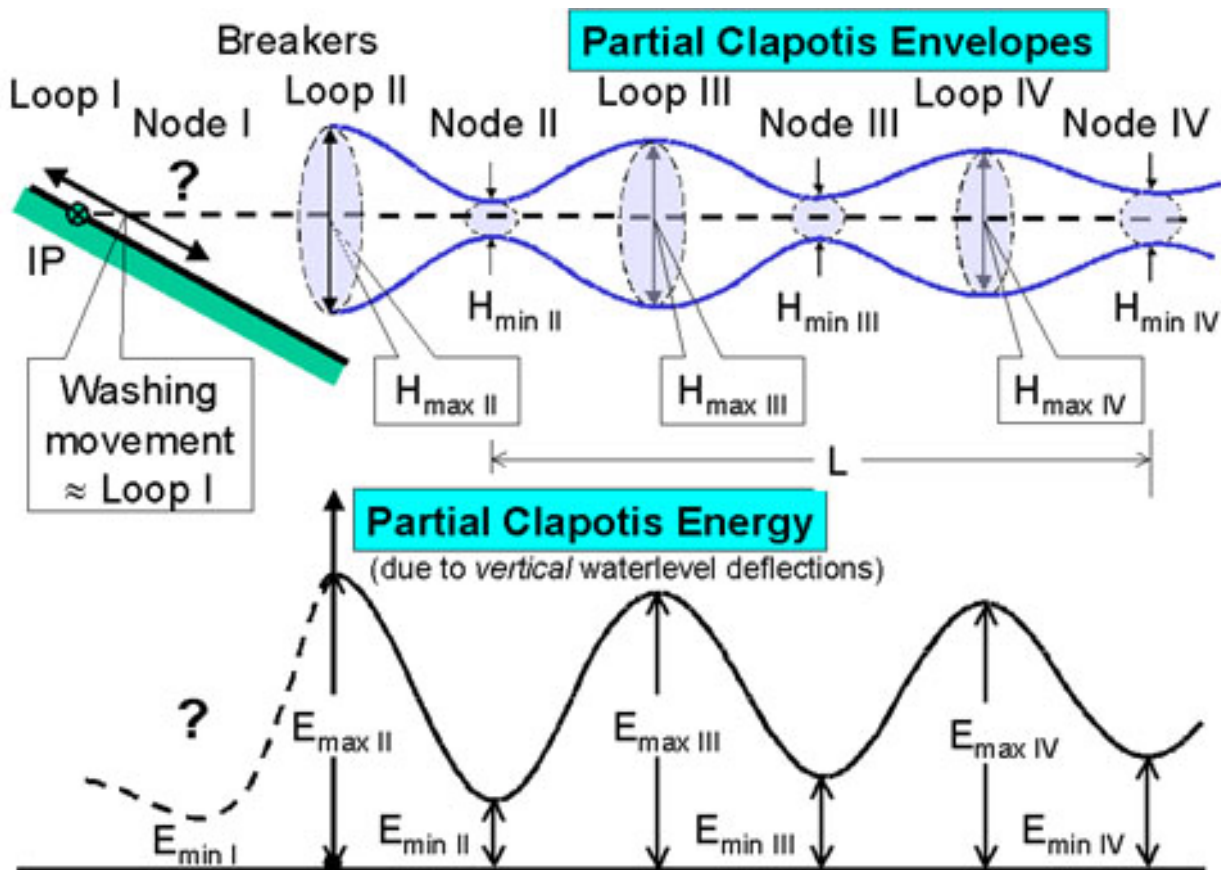


Fig.05: Generalized Water Level Envelopes and Energy of Partial Clapotis

In the next step of data evaluation all the energy amounts of such similar elementary frequency ranges were added up, reducing the number of curves to 12 only, see Fig.04.

Such curves obviously can be identified to be due to a set of partial clapotis. The *general* properties of any of those clapotis are to be seen in Fig.05.

In the lower part of that graph it is to be seen, that the absolute maximum of energy (denoted  $E_{\max II}$ ) appears closest to the slope and the seaward maxima  $E_{\max III}$ ,  $E_{\max IV}$  ... decrease in magnitude with the distance increasing from the slope. Vice versa with respect to the curve minima the energy increases with distance from the slope in the order  $E_{\min II}$ ,  $E_{\min III}$ ,  $E_{\min IV}$  ...

Obviously such features correspond very well to the water level envelopes of a partial standing wave attenuating with distance from IP, to be seen in the upper part of the graph. As wave energy  $E$  is proportional to the square of the wave heights  $H$ , previously reflection coefficients  $C_{R,i}$  had been extracted from the data of graphs, similar to that of Fig.04. Such data had been calculated previously in applying the formula

$$C_{R,i} = \frac{\sqrt{E_{\max,i}} - \sqrt{E_{\min,i}}}{\sqrt{E_{\max,i}} + \sqrt{E_{\min,i}}}, \text{ see [3] and [8]}$$

Where:

$E_{\max,i}$  = maximum energy of contributing components at clapotis loops,

$E_{\min,i}$  = minimum energy of contributing components at clapotis nodes,

$i$  = number of clapotis loops or nodes respectively.

Of course it is difficult to complete the graph of Fig.05 with respect to the breaking kinematics on the slope face. The only statements allowed in this context are: (1) Energy decreases in upslope direction depending on the type of breaker and on the slope angle. (2) The breaker extends from maximum Loop\_II to Node\_I. (3) Comparing particle movements on the slope to those at a vertical wall, the washing movement on the slope corresponds to Loop\_I (directly at the vertical wall face), although the runup can be compared better to a *broken* clapotis.

Starting from the assumption that a set of partial clapotis is present coincidentally in front of the sloping structure, cf. Fig.04, in the following some special results are found regarding the kinematics of breaking waves.

In Fig.06 some general changes are shown occurring in the case that the vertical wall is replaced by a sloping structure steeper than 1:3 [5]: Because of the vertical boundary missing, in those cases the perfect nodes con-

vert into imperfect nodes, whose centers are located appreciably nearer to IP than  $L/4$  (at a vertical wall). In the following evaluations are performed with respect to this feature on the smooth slope 1:3, based on the relative distances between the partial clapotis energy

lines of Fig.04. Here the longest component partial clapotis energy line is selected as a reference. This can be identified in the graph by its  $E_{\min II} \approx 0$  (nearly zero) at 3m from IP

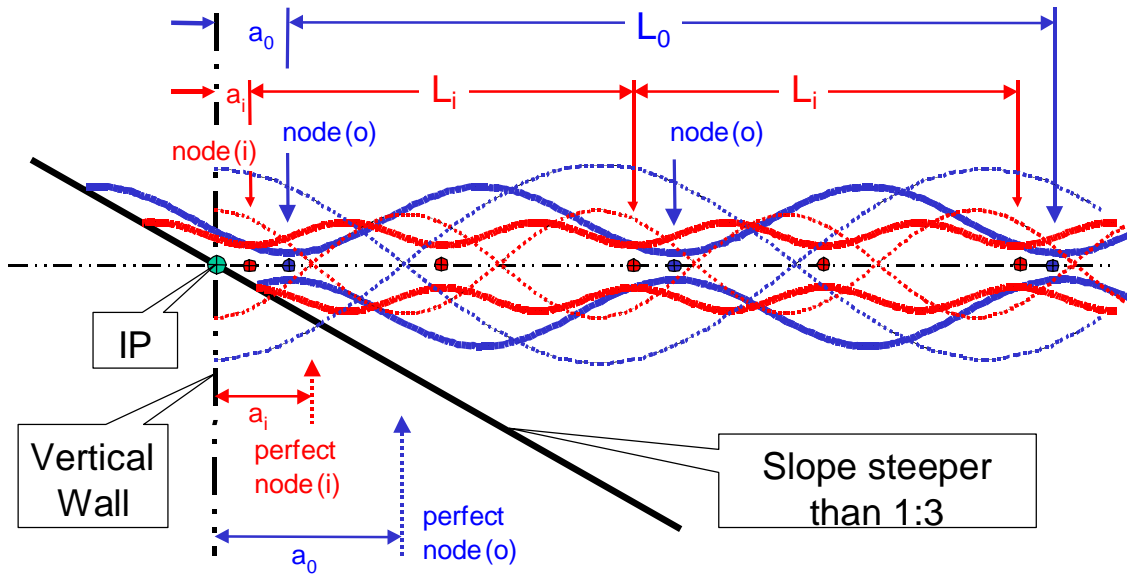


Fig.06: Two Sets of Partial Clapotis of Lengths  $L_0$  and  $L_i$  at a vertical wall and at a slope steeper than 1:3 respectively. Vertical wall: dotted lines; Smooth slope: solid lines.

### 3 Results

#### 3.1 Prebreaking Wave Stage

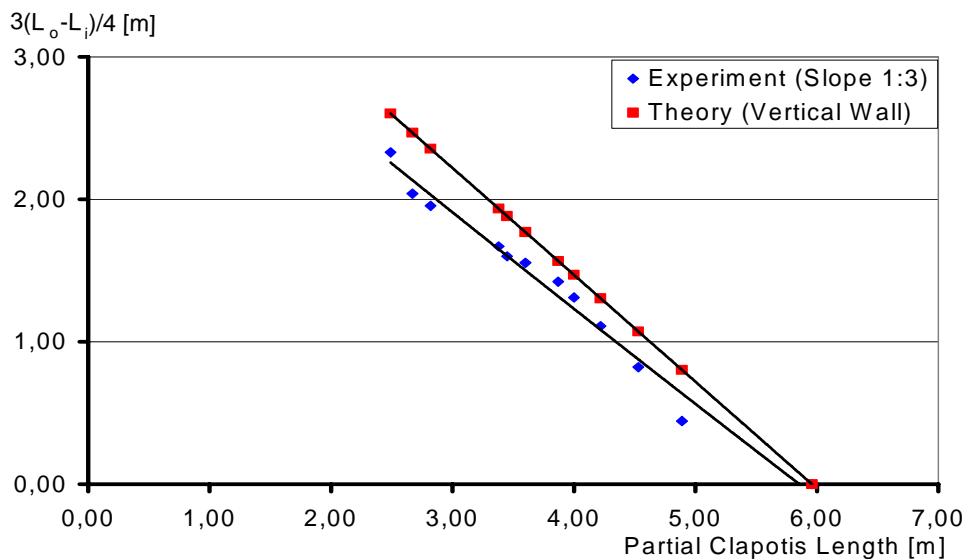


Fig.07: Distances of Partial Clapotis Nodes\_II with Reference to the Longest Partial Clapotis of Length  $L_0 = 6m$ .

In the process of wave deformation (at a slope) a *pre-breaking wave stage* obviously can be assigned to the position of node\_II ( $3L/4$  distant from vertical wall (IP)) of the longest clapotis component. In Fig.04 the respective location (of corresponding minimum energy of bound frequencies in the range  $0.4015 - 0.4232$  Hz) is the one mentioned above (3m from IP). The corresponding wave length is equal to the distance between  $E_{\min\text{III}}$  and  $E_{\min\text{IV}}$  resulting in approximately  $L_0 = 6\text{m}$ . Hence, in this case (of a slope structure) the distance of the node\_II from IP is only about  $2L/4$  (3m) instead of  $3L/4$  (4.5m). The distances from here to the nodes\_II of the remaining component clapotis waves are plotted in Fig.07. Comparing the results to the respective phase conditions at a vertical wall (theory), it can be seen that those distances decrease with the component frequency increasing (wave length decreasing). This means that in the *prebreaking* wave stage the steepening of the resul-

tant wave is due to the relative upsetting of partial clapotis component envelopes.

### 3.2 Breaking Wave Stage

Measurements could not be performed in using wave gauges on the slope face in the water depths region of the *breaking waves*, because of the minimum operational water depth not available here. Hence, in Fig.04 the loops\_II (maxima of energy) can be seen for the lower frequency partial clapotis only. It can, however, be supposed that at *wave breaking* the process of upsetting partial clapotis components is continued. The loops\_II of all clapotis components superimpose in such a way that an asymmetric distribution of energy is produced and stable surface elevations of the resultant waves can no longer be preserved. As to be seen from Fig.01 the asymmetry in the energy distribution with respect to the resultant partial clapotis is preserved also in the seaward wave cycles.

### 3.3 Postbreaking Wave Stage

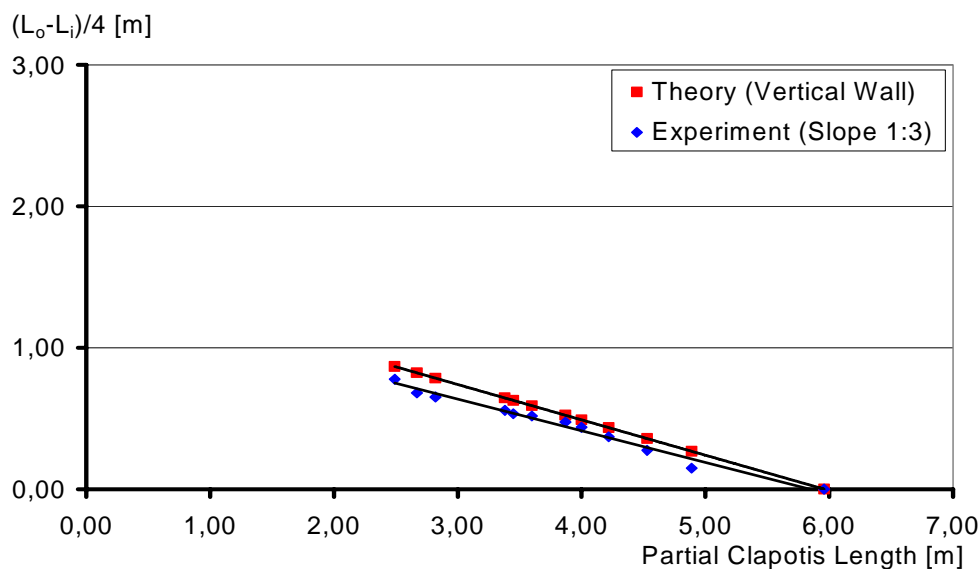


Fig.08: Distances of Clapotis Nodes\_I with Reference to Longest Partial Clapotis of Length  $L_0 = 6\text{m}$ .

Also the nodes\_I (at a distance of  $L/4$  from the vertical wall) of course can *not* be seen directly in Fig.04. Presuming, however, that partial clapotis lengths are constant on the slope, the locations of nodes\_I can be extrapolated in using the measured relative distances of the nodes\_II, shown in Fig.07. Similar to Fig.07 the extrapolated *relative* distances of clapotis nodes\_I with reference to those at a vertical wall (theory) are plotted in Fig.08. As the vertical scale is the same as in Fig.07, it is apparent that differences here are much smaller. This is also an indication that asymmetry changes with

the shifting of clapotis components. The absolute clapotis\_I node distances  $a_i$  from IP as defined in Fig.06 are shown in Fig.09 and the relative clapotis\_I node distances  $a_i/L_i$  with reference to IP in Fig.10.

The nodes\_I appear the more shifted in the upslope direction the higher the partial clapotis frequencies are. The negative values in Fig.09 and Fig.10 are plausible, because water particle movements extend in the upslope direction *beyond IP* and thus an increasing SWL - well known as wave setup - must exist. A similar result had

been obtained previously for monochromatic waves also, see [5]. It is apparent that the longest clapotis waves - though shifted with reference to their position at a vertical wall - feel the bottom at an appreciably larger relative distance from the structure than the shorter (higher frequency) clapotis waves do.

In the very vicinity of the slope face the actual positions of the nodes\_I with respect to the resultant breaker foot and *in the postbreaker kinematics* depend on the kind of breakers produced and on the frequencies contained in the partial clapotis.

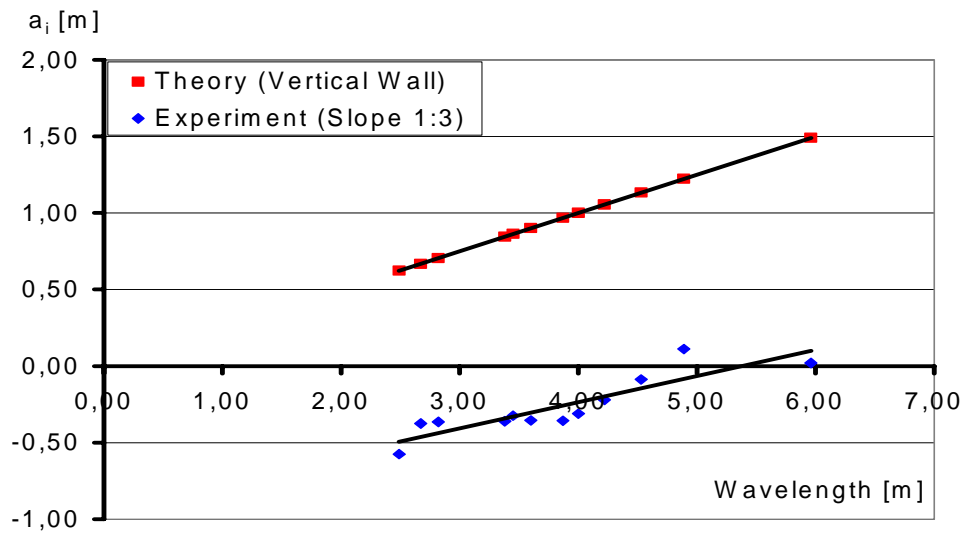


Fig.09: Absolute Clapotis Node\_I Distances from IP nearest to the Slope Face.

### 3.4 Washing Movement

The set of loops\_I (cf. Fig.05) can of course also *not* be seen from Fig.04. There is, however, some evidence,

that on a slope this feature of loops will be transferred into the washing movement (runup and rundown) of broken waves on the slope face.

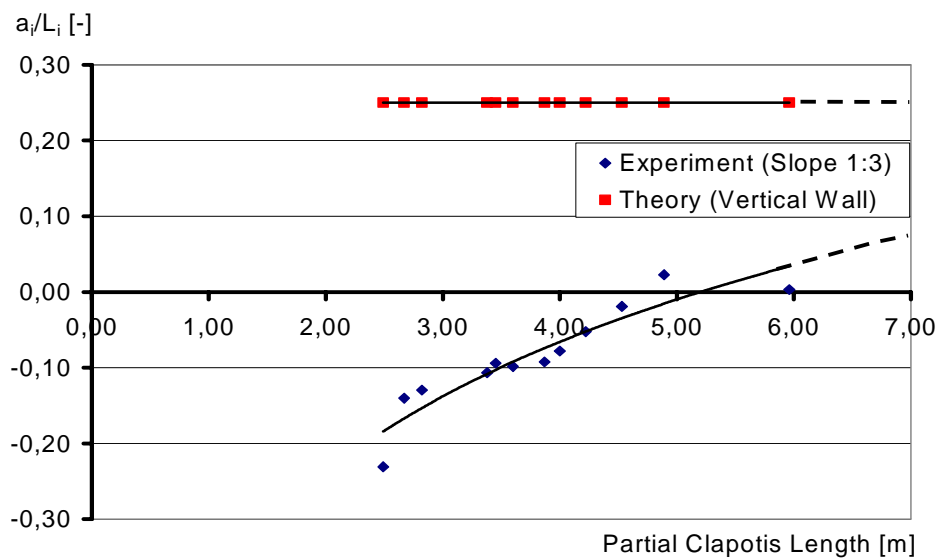


Fig.10: Relative Clapotis Node\_I Distances with Reference to IP.

## 4 Conclusions

In the theoretical treatment on reflection from a vertical wall, there is no additional dispersion to be considered, if water depth is big enough. In the case of a set of partial clapotis assumed to be present at a vertical wall, higher frequency partial clapotis should appear positioned nearer to IP, see Fig.06. There is, however, a big difference with respect to the particle kinematics at a sloping structure. In the case of the 1:3 slope combined effects of dispersion and reflection can be summarized as follows:

- Contrary to the refraction of a light spectrum into spectral colors by a prism of dispersion a similar splitting up of frequency components can be realized in the composite spectra of superimposed oncoming and reflected waves in front of a sloping structure.
- In the case that adjacent frequency components dispose of equal wave lengths a set of partial standing waves can be defined to be present coincidentally. Each of such bound frequency ranges (bound waves) are assigned by an anomalous dispersion property.
- The (composed) partial clapotis waves appear the more pronounced (by bigger reflection coefficients) the lower their mean frequencies.
- Compared to the vertical wall all superimposed component clapotis waves appear shifted in the up-slope direction with reference to IP.
- The relative shift increases with frequency and is in accordance with increasing asymmetry of the resultant breaking waves.

## 5 Acknowledgements

The author gratefully acknowledges the co-operation of Dipl.-Ing. D. Holtmann, Dipl.-Ing. K. Keull, Dipl.-Ing. W. Thienelt and F. Gerstendorf, in performing the model structures and helping to carry out the measurements at the Fluid Dynamics Laboratory of Bielefeld University of Applied Sciences.

## 6 References

- [1] Büsching, F.: „Durchströmbare Böschungsstrukturen“, *BAUINGENIEUR* 66 p.11-14, 1991
- [2] Büsching, F.: “Embankment Protection Structure”; *European Patent Office* Nr. 91103801.6-2303, 1991
- [3] Büsching, F.: “Wave and Downrush Interaction on Sloping Structures”, *Proc. 10th International Harbour Congress*, Antwerpen, Belgium, p. 5.17-5.25, 1992
- [4] Büsching, F.: “Imperfect Reflection from Permeable Revetment Structures”, *1st Int. Scientific Colloquium CAE TECHNIQUES*, p.177-189, Rzeszow, Poland, 1994

- [5] Büsching, F.: “Hollow Revetment Elements”, *COPEDEC IV*, Rio de Janeiro, Brazil, 1995
- [6] Büsching, F.: “On the Change of Reflection from Different Sloping Structures”, *2nd Int. Scientific Colloquium CAE TECHNIQUES*, p.305-314, Bielefeld, Germany, 1995
- [7] Büsching, F.: “On Energy Spectra of Irregular Surf Waves”, *Proc. 15th Int. Conf. on Coastal Eng.*, Honolulu, USA, 1976
- [8] Büsching, F.: “Reflection from Hollow Armour Units”, *COPEDEC V*, Cape Town, South Africa, 1999
- [9] Hagemeyer, K., Kramer, M.: „Reflexion irregulärer Wellen an geböschten Uferschutzbauwerken“, *Diplomarbeiten Bielefeld University of Applied Sciences* (1992), unpublished
- [10] Büsching, F.: <http://www.hollow-cubes.de>